In situ characterization of the deposition of anatase TiO$_2$ on rutile TiO$_2$(110)

Ashley R. Head, Niclas Johansson, Yuran Niu, Olesia Snezhkova, Shilpi Chaudhary, Joachim Schnadt, Hendrik Bluhm, Chaoyu Chen, José Avila, and Maria-Carmen Asensio

---

Articles you may be interested in

In situ characterization of the deposition of anatase TiO$_2$ on rutile TiO$_2$(110)

Ashley R. Head[a)] and Niclas Johansson
Division of Synchrotron Radiation Research, Department of Physics, Lund University, Box 118, 22100 Lund, Sweden

Yuran Niu[b)]
MAX IV Laboratory, Lund University, Box 118, 22100 Lund, Sweden

Olesia Snezhkova, Shilpi Chaudhary,[c)] and Joachim Schnadt[d)]
Division of Synchrotron Radiation Research, Department of Physics, Lund University, Box 118, 22100 Lund, Sweden

Hendrik Bluhm
Chemical Sciences Division and Advanced Light Source, Lawrence Berkeley National Laboratory, Berkeley, California 94720

Chaoyu Chen, José Avila, and Maria-Carmen Asensio
ANTARES Beamline, Synchrotron SOLEIL, Université Paris-Saclay, L'Orme des Merisiers, Saint Aubin-BP 48, 91192 Gif sur Yvette Cedex, France

Growing additional TiO$_2$ thin films on TiO$_2$ substrates in ultrahigh vacuum (UHV)-compatible chambers have many applications for sample preparation, such as smoothing surface morphologies, templating, and covering impurities. However, there has been little study into how to control the morphology of TiO$_2$ films deposited onto TiO$_2$ substrates, especially using atomic layer deposition (ALD) precursors. Here, the authors show the growth of a TiO$_2$ film on a rutile TiO$_2$(110) surface using titanium tetraisopropoxide (TTIP) and water as the precursors at pressures well below those used in common ALD reactors. X-ray absorption spectroscopy suggests that the relatively low sample temperature (175 °C) results in an anatase film despite the rutile template of the substrate. Using ambient pressure x-ray photoelectron spectroscopy, the adsorption of TTIP was found to be self-limiting, even at room temperature. No molecular water was found to adsorb on the surface. The deposited thickness suggests that an alternate chemical vapor deposition growth mechanism may be dominating the growth process. This study highlights the possibility that metal oxide film deposition from molecular precursors is an option for sample preparations in common UHV-compatible chambers. © *2018 Author(s). All article content, except where otherwise noted, is licensed under a Creative Commons Attribution (CC BY) license (http://creativecommons.org/licenses/by/4.0/).* https://doi.org/10.1116/1.5005533

I. INTRODUCTION

Thin film deposition of TiO$_2$ is routinely performed using methods such as atomic layer deposition (ALD), chemical vapor deposition (CVD), and pulsed laser deposition (PLD). These thin films are used in dye-sensitized solar cells[1] and other photocatalytic applications.[2] TiO$_2$ is easily deposited on different substrates in deposition reactors, with the choice of several molecular precursors.[3] Ways to control the morphology, impurity concentration, and crystalline phase using ALD are fairly well-known;[3] previous studies have shown that epitaxial growth of TiO$_2$ films is possible using ALD, CVD, and other deposition techniques on substrates with similar lattices, such as Al$_2$O$_3$ (0001),[4] SrTiO$_3$,[5–8] LaAlO$_3$,[9] RuO$_2$,[10] and SnO$_2$ nanowires.[11] In contrast, there are fewer investigations on the deposition of thin TiO$_2$ films on various TiO$_2$ substrates. Homoepitaxial films of both anatase and rutile TiO$_2$ have been grown on TiO$_2$ substrates using ALD,[12] PLD,[13,14] and molecular beam epitaxy,[15] but the growth of anatase TiO$_2$ on rutile TiO$_2$ via ALD has not been reported, to the best of our knowledge.

Depositing additional TiO$_2$ films onto TiO$_2$ substrates could potentially be useful in several applications. Surface defects or rough morphologies of a previously prepared surface could be repaired. Since it is difficult to grow bulk anatase TiO$_2$ crystals, naturally formed ones that contain impurities are used often in surface science studies,[16] and, in our experience, commercial rutile TiO$_2$ crystals can have Si or K contamination. Epitaxial growth of TiO$_2$ could cover such impurities. Complex surfaces could be synthesized by using a variety of templates, including molecules,[17] nanotemplates,[18] or patterned self-assembled monolayers[19] or polymers[20] to selectively deposit additional TiO$_2$ on a substrate. Mixed anatase/rutile TiO$_2$ materials and the interface between the two phases have shown enhanced photocatalytic behavior over one phase alone.[2] Understanding conditions for homoepitaxial and heteroepitaxial growth is important for such applications.

---

a)Present address: Chemical Sciences Division, Lawrence Berkeley National Laboratory, Berkeley, CA 94720.
b)Present address: School of Physics and Astronomy, Cardiff University, Cardiff CF24 3AA, United Kingdom.
c)Present address: Department of Physics, Indian Institute of Technology Ropar, Rupnagar, Punjab 140001, India.
d)Electronic mail: joachim.schnadt@sljus.lu.se

Of great interest in the surface science community are spectroscopic and microscopic studies of pristine surfaces, largely conducted in ultrahigh vacuum (UHV) conditions. Investigations of the adsorption of ALD precursors on surfaces are commonplace, but there are few studies of CVD processes[21–24] and cyclic processes of ALD in UHV-compatible chambers.[25–28] Feasibility of such deposition could offer a new option to grow materials in UHV-compatible chambers, including a way to obtain a smooth or impurity-free surface, especially when fairly low temperatures during the deposition are required. Here, we investigate the deposition of TiO₂ from two common deposition precursors,[29–31] titanium tetraisopropoxide (TTIP) and water, on a rutile TiO₂(110) crystal at 175 °C, where a series of ligand exchange reactions is the known reaction mechanism on the surface at this temperature under precursor pressures common to industrial ALD.[30] Using ambient pressure x-ray photoelectron spectroscopy (APXPS), the surface species during precursor dosing are monitored in a semiquantitative manner over a range of pressures up to 0.014 Torr. In this context, it should be noted that APXPS is distinguished from *in situ* XPS, where an ALD apparatus is connected through vacuum to an XPS instrument; in that case, the surface species are monitored in UHV *after* precursor exposure. X-ray adsorption spectroscopy (XAS) is used to determine that the film does not continue in the rutile phase. Low-energy electron diffraction (LEED) and atomic force microscopy (AFM) show the corrugated morphology of a film grown with ten precursor dosing cycles. The apparent thickness of the film is much larger than would be expected for standard ALD ligand exchange mechanisms and could be consistent with a CVD growth mechanism seen by Johnson and Stair in a similar study of TiO₂ deposition on MoOₓ.[25]

II. EXPERIMENT

A. Ambient pressure XPS

The experiments were performed at the APXPS end station[32] of beamline 11.0.2 (Ref. 33) at Lawrence Berkeley National Laboratory's Advanced Light Source. A rutile TiO₂(110) crystal (SurfaceNet GmbH, Germany) was cleaned with cycles of Ar^+ sputtering (1 keV, 5×10^{-6} mbar, 5 mA) and annealing to 620 °C until no carbon was detected in the x-ray photoelectron (XP) spectra. The deposition was performed by introducing alternating pressures of TTIP (99.999%, Sigma-Aldrich) and water in the analysis chamber via a precision leak valve. In contrast to industrial ALD reactors, no carrier gas was used. Instead of inert purging steps, evacuation of the precursors was performed. The pressures are mentioned in the text. As discussed below, the experimental chamber is difficult to restore to UHV conditions after dosing TTIP in the mTorr regime without a standard UHV bakeout; however, dosing at lower pressures (1×10^{-6} Torr and below) allowed for recovery of UHV conditions without background TTIP after a day of standard pumping of the analysis chamber. Several experiments were conducted with the same crystal. Sputter and anneal cycles were always performed before each new series of

experiments. Occasionally, depending on the background conditions, introducing our TiO₂ crystal into the analysis chamber resulted in immediate reaction with background TTIP. All spectra shown below were collected starting with a clean, carbon-free surface immediately prior to dosing TTIP. However, the data plotted in Fig. 2 are from an experiment that did contain TTIP on the initial surface. This experimental iteration was chosen because it had the most precursor dosing cycles and contains peak area changes that are representative of all experiments.

Unless mentioned otherwise, the sample was kept at 175 °C during dosing, as monitored by a K-type thermocouple. The spectra were referenced to the Fermi level of gold foil in good ohmic contact with the titania crystal. A polynomial background was removed from the spectra. A least squares fitting analysis was used with Voigt functions. The combined resolution of the beamline and the electron energy analyzer was better than 0.30 eV. In order to minimize damage to the molecules from the photon beam, each spectrum was collected on a new area of the sample and the collection time of each spectrum was minimized. More information on the observed photon-induced effects is given in Sec. S1 of the supplementary material.[44]

B. X-ray absorption spectroscopy

A TiO₂ film was deposited on a clean rutile TiO₂(110) crystal by performing ten precursor dosing cycles (each half-cycle used a precursor pressure of 1×10^{-7} Torr for 10 min at 175 °C). The sample was transported *ex situ* to the experimental chamber of the ANTARES beamline (Synchrotron SOLEIL, France),[34] where it was heated to 200 °C in vacuum at a pressure lower than 1×10^{-9} mbar. The spectra were collected in three modes: total electron yield (TY), partial electron yield (PY), and fluorescence yield (FY). In the partial electron yield, both the O K-edge and the Ti L-edge were collected with a 2 eV kinetic energy window centered at 15 eV. The photon energy was calibrated by taking the difference in kinetic energy of a suitable XPS line excited by first and second order photons transmitted by the beamline's monochromator.

C. LEED

A TiO₂ film was deposited as for the XAS study and examined *in situ* using micro-low-energy electron diffraction (μ-LEED) in an ACLEEM instrument (Elmitec GmbH) at beamline I311 on the MAX II storage ring of the MAX IV Laboratory (Lund, Sweden). The film was removed and examined using *ex situ* AFM.

III. RESULTS

A. Spectroscopy

Aspects of the surface chemical reactions of the deposition of TiO₂ from TTIP and water were investigated by collecting XP spectra while dosing the precursors on a rutile TiO₂(110) surface. Figure 1(a) shows the C 1s spectra while dosing TTIP at 1×10^{-5} Torr at 150 °C and at 0.014 Torr at
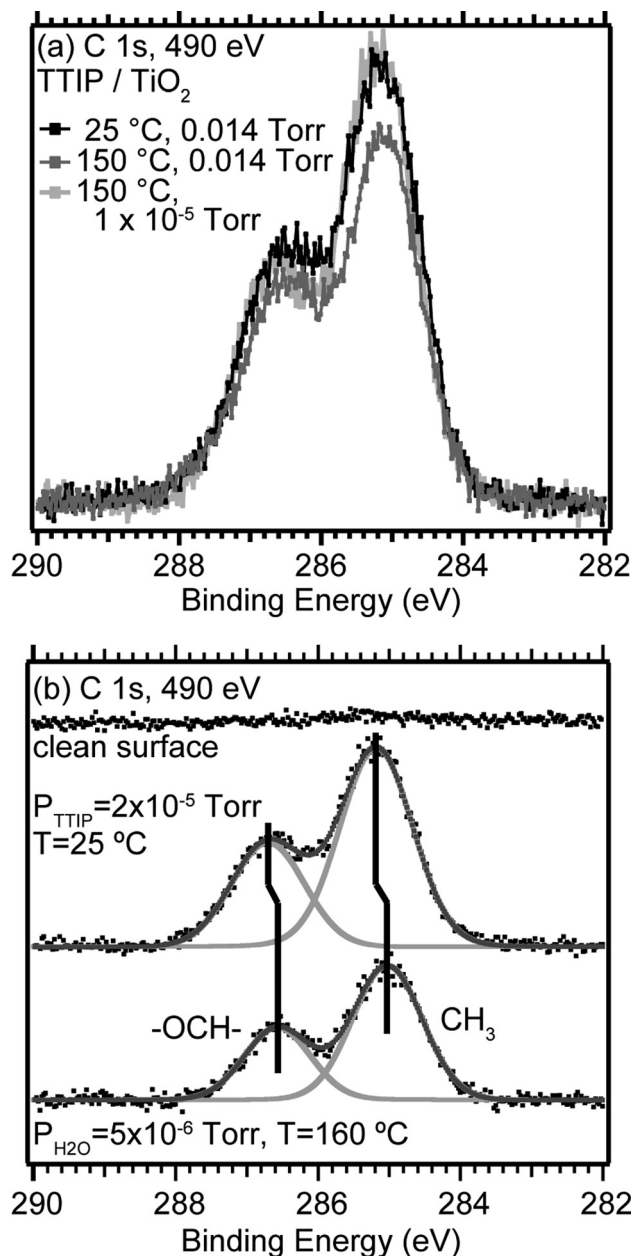
FIG. 1. C 1s spectra at (a) different substrate temperatures and TTIP pressures: 0.014 Torr at 25 °C (black) and 150 °C (gray) and 1×10^{-5} Torr at 150 °C (light gray). (b) C 1s spectra immediately before dosing TTIP (top), and at pressures of 1×10^{-5} Torr TTIP (middle) and 5×10^{-6} Torr H$_2$O (bottom), all at 175 °C. The black dots are the collected data, and the dark line is a fit of Voigt functions (gray). The solid black line indicates a shift of 150 meV for both peaks.

150 and 25 °C. The similar intensity of the C 1s spectra in Fig. 1(a) shows no pressure or temperature dependence on TTIP adsorption in this pressure regime. The increase in binding energy that often accompanies multilayer formation is also absent. The C 1s spectra agree with previous studies of surface-bound TTIP (Refs. 24 and 25) and are fit with two peaks in Fig. 1(b). The larger peak at 285.19 eV is the ionization from the methyl carbons, and the smaller peak at 286.70 eV is from the –OCH- group. The area ratio of the peaks is 2 CH$_3$:1 –OCH-, as in the intact molecule. Once water is dosed, the amount of carbon decreases and both C

1s peaks shift by 150 meV toward lower binding energy, as seen in Fig. 1(b). This shift is cyclic and occurs in the three dosing cycles that were monitored.

Figure 2 details the cyclic changes in the C 1s intensity. Initially, a background pressure of TTIP results in a significant amount of carbon on the surface, but the coverage is not saturated since the intensity increases upon dosing at 1×10^{-5} Torr. Upon dosing water at a pressure of 5×10^{-6} Torr, more than half of the carbon remains. Evacuation of the water removes more carbon, and it is difficult to distinguish between nonideal ALD behavior and adsorption of TTIP lingering in the background.

Figure 3(a) shows the O 1s spectrum of the clean TiO$_2$ substrate, with the large gray peak from the bulk oxygen signal and the small light gray peak from surface hydroxyl groups.[35] The TTIP exposure [Fig. 3(b)] attenuates the bulk signal, and the signal from the isopropyl group of the TTIP appears as a broad component at 531.4 eV. During the water dosing [Fig. 3(c)], the signal from the hydroxyl groups at 531.8 eV (Ref. 35) overlaps with the peak of the isopropyl groups that remain. With removal of some isopropyl groups, the attenuation of the bulk oxide peak lessens. Notably absent from the O 1s spectrum during the water exposure is a signal from absorbed molecular water around a binding energy of 534 eV.[35,36] The Ti 2p$_{3/2}$ spectrum of the clean TiO$_2$ is shown in Fig. 4. The low binding energy shoulder indicates Ti^{3+} at oxygen vacancy sites.[16] After three full precursor dosing cycles, the intensity of the Ti^{3+} shoulder is reduced in comparison to the starting surface, indicating a filling or covering of the defects.

To determine if the crystal structure of the deposited TiO$_2$ film was continuing the rutile phase of the TiO$_2$ substrate, Ti L-edge and O K-edge XAS data were collected on a film grown from ten precursor dosing cycles. Using three detectors simultaneously, the absorption spectra (Fig. 5) were
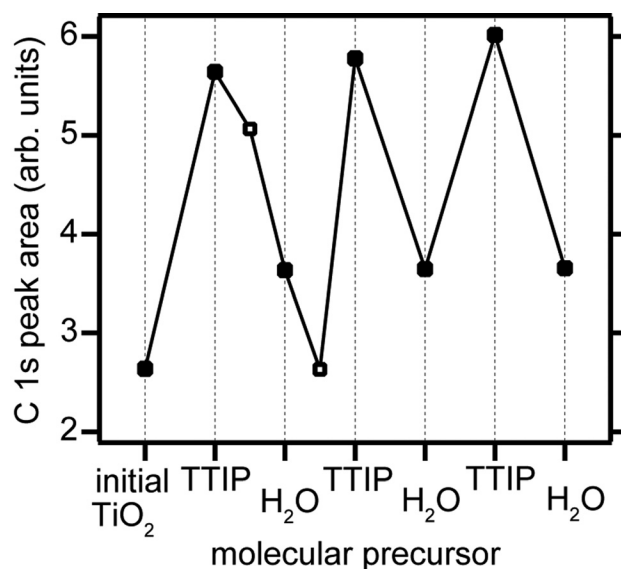

FIG. 2. C 1s peak area of the cleaned TiO$_2$ and during each precursor dosing, where the pressure of TTIP was 1×10^{-5} Torr and the pressure of water was 5×10^{-6} Torr. The open squares are after evacuation of the precursor with a base pressure of 1×10^{-7} Torr. The error for each point is not larger than 0.12.
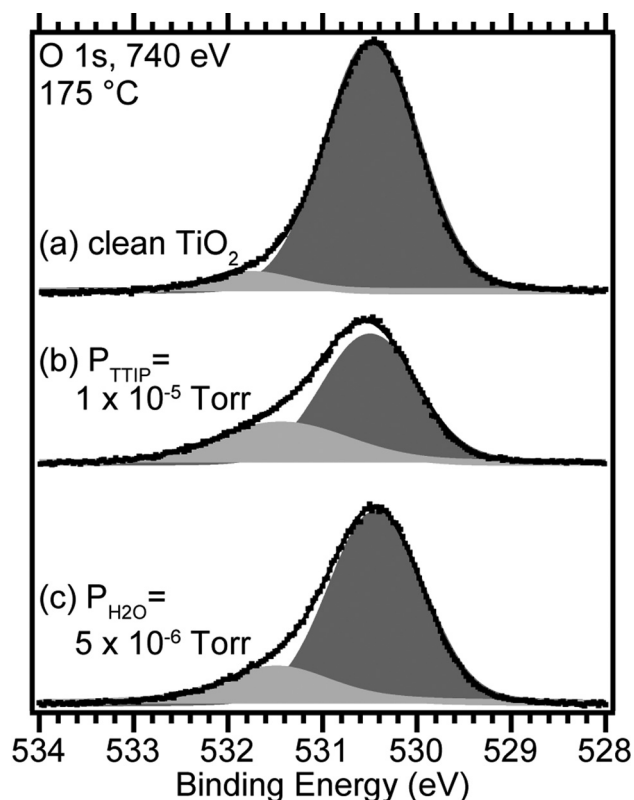
FIG. 3. O 1s spectra of (a) clean TiO_2, (b) during a TTIP pressure of 1×10^{-5} Torr, and (c) during a water pressure of 5×10^{-6} Torr. The darker peak represents the bulk signal, and the lighter peak represents (a) surface hydroxyl groups, (b) isopropoxyl ligands, and (c) a combination of isopropoxyl ligands and hydroxyl groups.

FIG. 4. Ti $2p_{3/2}$ XP spectra of the clean TiO_2 (black) and after three complete precursor dosing cycles (gray). The spectra are normalized to their maximum heights.

collected in three modes with different surface sensitivities: partial electron yield, total electron yield, and fluorescence yield. In the more surface-sensitive partial and total yield modes, the intensities of the peaks at 459.5 and 460.5 eV in the Ti absorption spectra are similar to that of anatase TiO_2, shown in the top spectrum of Fig. 5(a). The relatively more bulk-sensitive fluorescence mode spectrum in Fig. 5(a) looks less anatase and is likely a mixture of signals from both the surface anatase and the rutile bulk. The phase depicted in the O absorption spectra is more difficult to discern in Fig. 5(b). The fluorescence yield Ti L-edge data are rather noisy, especially compared with those of the O K-edge; the higher signal in the O spectrum is due to the increased probability of fluorescence.[37]

B. Morphology characterization

The morphology of the thicker film grown with ten precursor dosing cycles was also investigated. Without exposing the sample to the atmosphere, a low energy electron diffraction image was collected using μ-LEED. μ-LEED was used here because a typical LEED with a larger beam size damaged the film too quickly and produced the LEED pattern of the substrate only. Figure 6 shows a μ-LEED image that is similar to that of a clean rutile $TiO_2(110)$ (1×1) surface, except that four spots are missing, as indicated with the white circles. The weak intensity, especially the disappearances, can indicate that the film growth is not homogenous.
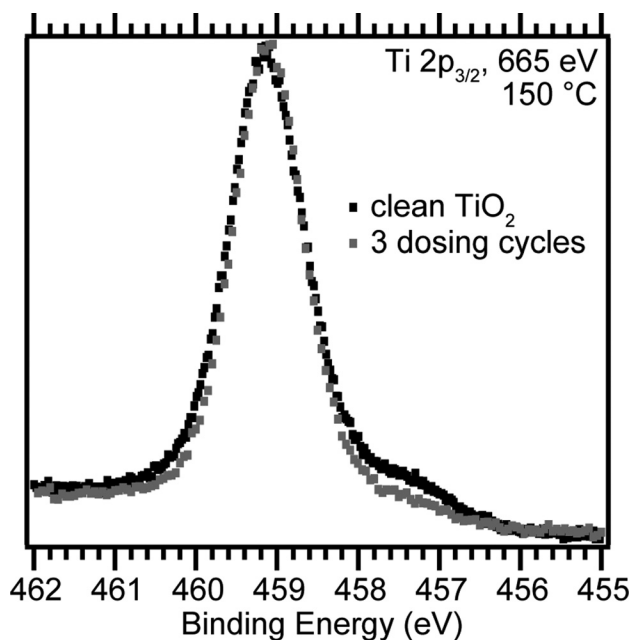
After about two minutes of exposure to the electron beam, the film is damaged and the missing spots reappear, yielding the diffraction pattern of the substrate [Fig. 6(b)]. Comparison between *ex situ* AFM images of the rutile crystal and the deposited film [Figs. 7(a) and 7(b), respectively] shows a corrugated film that agrees with this interpretation of the LEED.

IV. DISCUSSION

A. Deposition process

The precursor dosing during the deposition of TiO_2 from TTIP and H_2O was monitored using APXPS. In comparison to standard deposition processes, no carrier gas was used. Additionally, instead of an inert gas purge step that is used in ALD, the precursors were evacuated. The standard UHV experimental chamber used is not designed to have a gas flow across the sample; thus, it is unlikely that an inert gas purge step would be more effective than precursor evacuation. Some APXPS instrumentation is designed with a gas flow in front of the sample,[38] and the effect of a purge step in such a setup would be a feasible experiment.

Previous reports show that TTIP absorbs to a surface in a self-limiting fashion independent of pressure in the temperature range of 100–250 °C.[31] The C 1s spectra in Fig. 1(a) confirm that this behavior is also true down to 25 °C and up to 0.014 Torr. This result lies in contrast with the study of TTIP on MoO_x where no evidence of TTIP adsorption on room temperature MoO_x was found in XPS data.[25] Interestingly, there is a reproducible shift in the C 1s binding energies between the dosing of the different precursors [Fig. 1(b)]. Band bending effects do no generate this shift since the other core levels remain constant. This binding energy decrease could be due to stabilizing effects of intermolecular
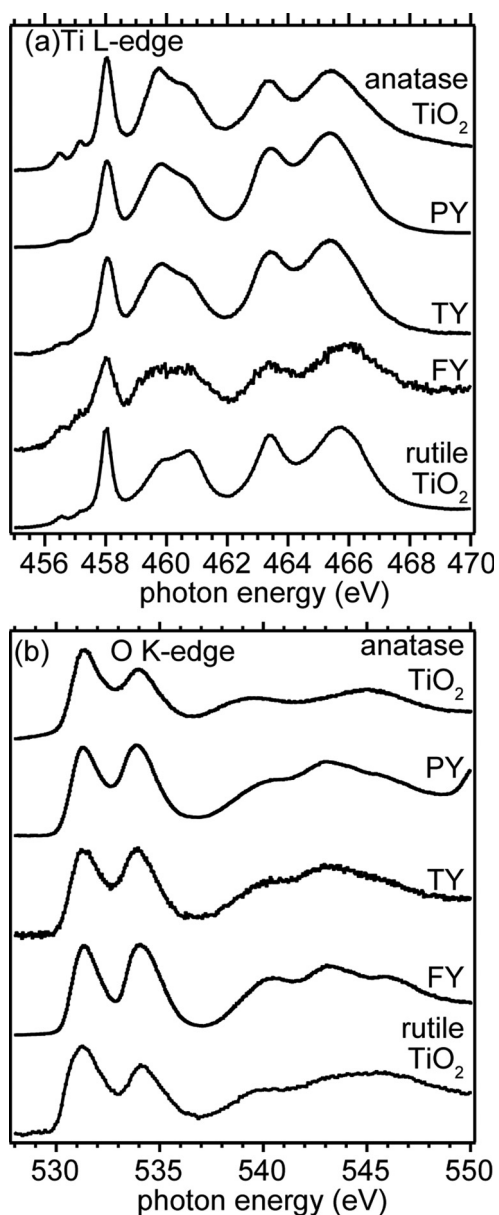
FIG. 5. (a) Ti L-edge and (b) O K-edge absorption spectra of a TiO$_2$ film deposited with ten precursor dosing cycles onto a rutile TiO$_2$(110) substrate. The spectra collected with PY, TY, and FY detectors are shown. Rutile and anatase TiO$_2$ spectra are shown for comparison. The spectra are normalized to their maximum height.

FIG. 6. (a) μ-LEED image of a film grown with ten complete precursor dosing cycles on a rutile TiO$_2$(110) surface shows missing spots (circles) for a typical (1 × 1) LEED pattern that reappears after 2 min under the electron beam (b). The size of the LEED electron beam is about 5 μm, and the energy is 40 eV.

interactions between the large isopropoxide groups; as the isopropoxide ligands are replaced by hydroxyl groups, the remaining, less sterically hindered ligands may be able to more effectively screen the positive photohole. A second possibility is anchored in initial state effects. The more electron-rich hydroxyl groups will push more electron density onto the Ti atom and slightly to the isopropoxide ligand, decreasing the C 1s binding energy. However, it is unclear if such a subtle change in ligands would indeed cause a binding energy shift. The bulkier isopropoxide group would be more efficient at screening a charge, which may cancel any binding energy decrease from an initial state effect. Unfortunately, there is little literature on such binding energy shifts. Some insight can be gleaned from Si 2p binding energy shifts of similar
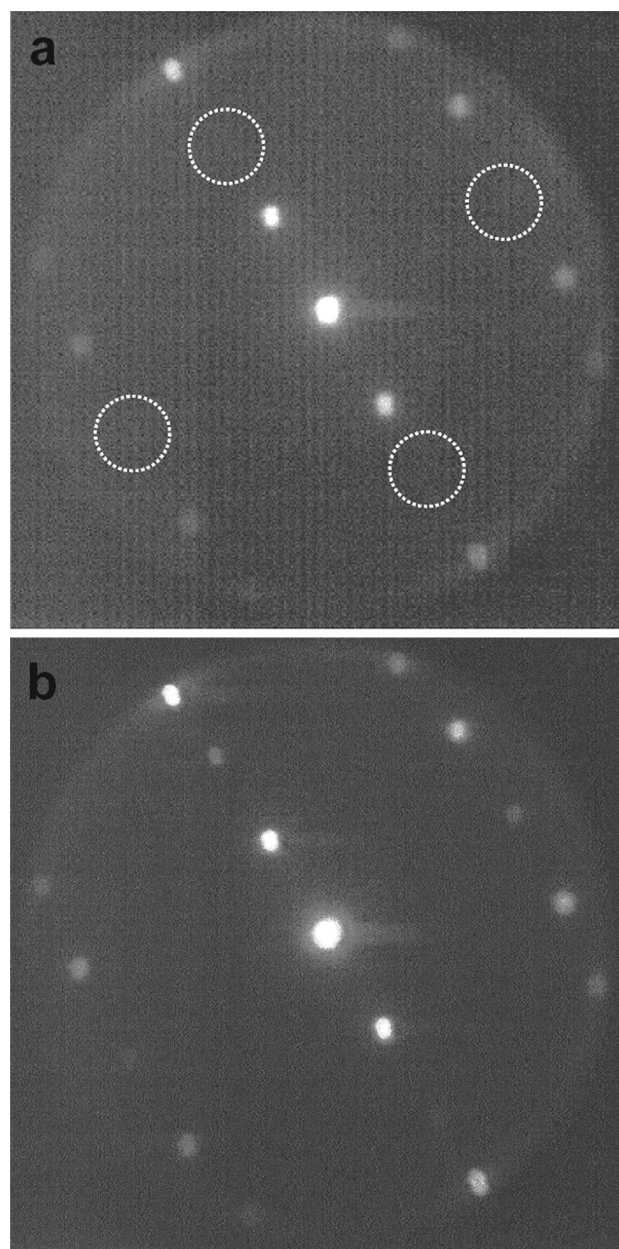
systems. Upon comparing hydroxyl groups on Si (100)[39] and ethoxy groups on Si (111),[21] the binding energy of the surface Si atoms shifts by +0.9 eV upon binding to either group (i.e., the hydroxyl and ethoxy groups donate the same amount of electron density to Si). Furthermore, final state effects are responsible for the increased Si 2p binding energy of tetra-methoxysilane (170.70 eV) compared to tetraethyoxysilane (107.56 eV).[40] Thus, it is unclear if the extra electron density provided by the hydroxyl group would be sufficient to overcome screening effects by the isopropoxide ligands in our system.

From quartz crystalline microbalance studies, it has been calculated that about 2.2–2.5 ligands leave per TTIP adsorption on the surface during the standard ALD mechanism;[29,31]
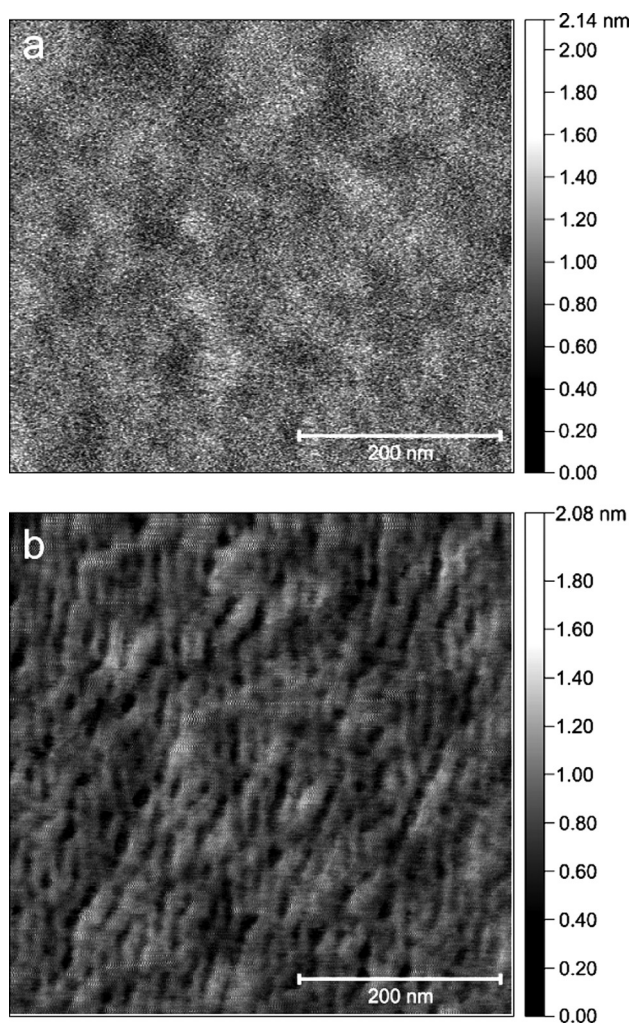
FIG. 7. AFM images of the rutile TiO_2 crystal (a) before and (b) after deposition of TiO_2 with ten precursor dosing cycles.

coverage calculations in the current study are difficult since the film and the substrate are the same material. Previous studies have shown that water does not remove all the isoproxide ligands from the surface, suggesting that 30% of the ligands remain.[31] A background pressure of TTIP in the analysis chamber prevents quantification of the amount of isopropyl groups remaining on the surface, as there could be mixing between the precursors. The amount of carbon on the surface upon immediate introduction of the sample into the analysis chamber and after evacuation of the water indicates that the background TTIP pressure is significant. However, when dosing TTIP and water in a more controlled UHV environment at lower pressures, where mixing between the precursors in the gas phase is not expected, the water still does not remove all the isopropyl ligands (see Fig. S4). Furthermore, Lee and coworkers reported that carbon remained on the surface throughout the ALD process after water exposure.[41] It has been suggested that longer exposures to water could remove more carbon;[31] however, we did not see such behavior, even up to a pressure of 0.080 Torr of water (see Fig. S3).

Johnson and Stair reported that a CVD mechanism dominates the deposition process at low precursor pressures (at and lower than 3×10^{-6} Torr) at $100\,°C$ on a MoO_x substrate.[25]

Their analysis is based on the quantification of Ti and C XPS data. The mechanism proposes dehydration of the isoproxide ligand on the Ti sites. The low TTIP flux at a modest temperature is thought to slow the kinetics of the ALD process enough to allow the alternative CVD process to occur. With the substrate and the film material being the same in our study, quantification of Ti and C on the surface is challenging. Since the dehydration occurs on a Ti site, it is feasible that the low-temperature CVD could occur on our TiO_2 substrate.

B. Thin film properties

The morphology of the film shows a corrugated surface, as seen in the AFM image in Fig. 7(b). The uneven thickness in the AFM image can explain the missing spots in the LEED pattern. A film with ordered atoms but containing surface imperfections, such as uneven layers, can cause a decrease in LEED spot intensities.[42]

It is challenging to estimate the thickness of the film since the substrate and the film are the same material. Using a growth per cycle of 0.05 nm/cycle from a typical ALD study,[31] a lower limit to the film thickness can be estimated to be about 0.5 nm. With the background TTIP and water pressures in the chamber during the experiments, it is likely that the film is even thicker, and XAS data, indeed, point toward a larger thickness. Quantitative analysis of XAS data is difficult, but the nearly complete anatase fingerprint in the partial and total electron Ti L-edge spectra [Fig. 5(a)] indicates that the film extends almost the entire probing depth of the detection methods, which is on the order of 10 nm for semiconductors using total electron yield.[37] A thickness of 10 nm is not attainable from a purely ALD process. This thickness implies that there is an extensive precursor overlap that increases the growth or that the low-temperature CVD mechanism reported by Johnson and Stair is occurring.[25]

The fluorescence yield spectrum probes deeper into the bulk (on the order of 50–100 nm),[37] and so, a larger rutile TiO_2 contribution is apparent and dampens the anatase profile in the Ti L-edge spectrum. With such a deep probing depth, the lack of a more distinct rutile spectrum in the fluorescence yield also hints at a thicker anatase film. An amorphous morphology can be excluded since the region between 459 and 463 eV would be a featureless peak with no discernable splitting.[43] Because absorption spectra of the anatase and rutile phases have less distinct features in the O adsorption spectrum, it is more challenging to identify the phase in the spectra. The O K-edge fluorescence yield spectrum is clearly rutile with three distinct peaks around 540, 543, and 546 eV; this result matches the rutile phase seen in the Ti L-edge spectrum. These rutile peaks are also present in the partial and total yield spectra, but they are less distinct. It is unclear if the indeterminate nature of the peaks is due to the sample collection method (position of the detector, incident angle of the photons, etc.) or if the anatase phase of the film is dampening the rutile signature.

The crystal structure of deposited TiO_2 depends on the deposition temperature, molecular precursors, and substrate.[3] Generally, for TTIP and water on metal oxide substrates,

amorphous films are grown for temperature ranges below ~150 °C.[3,31] Polycrystalline films occur above 180 °C (Ref. 31) with anatase being more common at lower temperatures and rutile prominent above ~250 °C.[3] Despite having a rutile template in this study, the temperature appears to be the dominating factor of the crystalline phase. In previous studies, rutile TiO₂ was homoepitaxially deposited onto rutile substrates at temperatures greater than 200 °C.[10,12–14]

V. CONCLUSIONS

Depositing TiO₂ at 175 °C using alternating TTIP and H₂O dosing with pressures at and below 1×10^{-5} Torr resulted in a film that appears to be anatase from the Ti L-edge XAS data. Despite the rutile template of the substrate, the temperature may be the prevailing factor in determining the crystalline phase. The XAS suggest a film thickness of at least 10 nm, which is unrealistic for ten ideal ALD cycles; the large thickness suggests that a CVD mechanism could play a dominate role in the deposition. The film morphology was found by AFM and μ-LEED to be corrugated. Using APXPS, the adsorption of TTIP was independent of pressure, even at room temperature. Molecular water adsorption on the surface was not detected. This study builds on our previous investigations of ALD (Ref. 27) and CVD (Ref. 21) with APXPS by showing that a film can be grown by dosing molecular precursors in a conventional UHV chamber using precursor pressures lower than typical industrial deposition reactors. APXPS experiments of ALD and CVD processes could be further improved by using a setup that has a smaller volume of gas and a gas flow over the sample;[38] precursor mixing could be avoided, and a purge step could be effectively introduced. Overall, this study highlights the potential of using synchrotron techniques in understanding fundamental reactions of deposition processes and characterizing the phase of film growth.

ACKNOWLEDGMENTS

[1]L. Alibabaei, B. H. Farnum, B. Kalanyan, M. K. Brennaman, M. D. Losego, G. N. Parsons, and T. J. Meyer, Nano Lett. **14**, 3255 (2014).

[2]L. Liu and X. Chen, Chem. Rev. **114**, 9890 (2014).

[3]V. Miikkulainen, M. Leskelä, M. Ritala, and R. L. Puurunen, J. Appl. Phys. **113**, 021301 (2013).

[4]K. Vasu, M. B. Sreedhara, J. Ghatak, and C. N. R. Rao, ACS Appl. Mater. Interfaces **8**, 7897 (2016).

[5]T. J. Kraus, A. B. Nepomnyashchii, and B. A. Parkinson, J. Vac. Sci. Technol., A **33**, 01A135 (2015).

[6]M. D. McDaniel, A. Posadas, T. Q. Ngo, A. Dhamdhere, D. J. Smith, A. A. Demkov, and J. G. Ekerdt, J. Vac. Sci. Technol., B **30**, 04E111 (2012).

[7]M. D. McDaniel, A. Posadas, T. Wang, A. A. Demkov, and J. G. Ekerdt, Thin Solid Films **520**, 6525 (2012).

[8]D. E. Barlaz and E. G. Seebauer, J. Vac. Sci. Technol., A **34**, 020603 (2016).

[9]Z. Zhang, L. M. Wong, Z. Zhang, Z. Wu, S. Wang, D. Chi, R. Hong, and W. Yang, Appl. Surf. Sci. **355**, 398 (2015).

[10]S. K. Kim, G. W. Hwang, W.-D. Kim, and C. S. Hwang, Electrochem. Solid-State Lett. **9**, F5 (2006).

[11]A. Nie *et al.*, J. Mater. Chem. **22**, 10665 (2012).

[12]T. J. Kraus, A. B. Nepomnyashchii, and B. A. Parkinson, ACS Appl. Mater. Interfaces **6**, 9946 (2014).

[13]Y. Yamamoto, Y. Matsumoto, and H. Koinuma, Appl. Surf. Sci. **238**, 189 (2004).

[14]S. Takata, R. Tanaka, A. Hachiya, and Y. Matsumoto, J. Appl. Phys. **110**, 103513 (2011).

[15]G. Herman and Y. Gao, Thin Solid Films **397**, 157 (2001).

[16]U. Diebold, Surf. Sci. Rep. **48**, 53 (2003).

[17]C. P. Canlas *et al.*, Nat. Chem. **4**, 1030 (2012).

[18]J. Y. Woo, H. Han, J. W. Kim, S.-M. Lee, J. S. Ha, J. H. Shim, and C.-S. Han, Nanotechnology **27**, 265301 (2016).

[19]F. S. M. Hashemi, B. R. Birchansky, and S. F. Bent, ACS Appl. Mater. Interfaces **8**, 33264 (2016).

[20]E. Färm, M. Kemell, M. Ritala, and M. Leskelä, J. Phys. Chem. C **112**, 15791 (2008).

[21]S. Chaudhary *et al.*, J. Phys. Chem. C **119**, 19149 (2015).

[22]C. J. Taylor, D. C. Gilmer, D. G. Colombo, G. D. Wilk, S. A. Campbell, J. Roberts, and W. L. Gladfelter, J. Am. Chem. Soc. **121**, 5220 (1999).

[23]M. Reinke, Y. Kuzminykh, and P. Hoffmann, J. Phys. Chem. C **119**, 27965 (2015).

[24]P. G. Karlsson, J. H. Richter, M. P. Andersson, M. K.-J. Johansson, J. Blomquist, P. Uvdal, and A. Sandell, Surf. Sci. **605**, 1147 (2011).

[25]A. M. Johnson and P. C. Stair, J. Phys. Chem. C **118**, 29361 (2014).

[26]P. C. Roy, H. S. Jeong, W. H. Doh, and C. M. Kim, Bull. Korean Chem. Soc. **34**, 1221 (2013).

[27]A. R. Head, S. Chaudhary, G. Olivieri, F. Bournel, J. N. Andersen, F. Rochet, J.-J. Gallet, and J. Schnadt, J. Phys. Chem. C **120**, 243 (2016).

[28]A. Lemonds, J. White, and J. Ekerdt, Surf. Sci. **538**, 191 (2003).

[29]A. Rahtu and M. Ritala, Chem. Vap. Deposition **8**, 21 (2002).

[30]M. Reinke, Y. Kuzminykh, and P. Hoffmann, Chem. Mater. **27**, 1604 (2015).

[31]J. Aarik, A. Aidla, T. Uustare, M. Ritala, and M. Leskelä, Appl. Surf. Sci. **161**, 385 (2000).

[32]D. Frank Ogletree, H. Bluhm, E. D. Hebenstreit, and M. Salmeron, Nucl. Instrum. Methods Phys. Res., Sect. A **601**, 151 (2009).

[33]H. Bluhm *et al.*, J. Electron Spectrosc. Relat. Phenom. **150**, 86 (2006).

[34]C. Chen, J. Avila, E. Frantzeskakis, A. Levy, and M. C. Asensio, Nat. Commun. **6**, 8585 (2015).

[35]G. Ketteler, S. Yamamoto, H. Bluhm, K. Andersson, D. E. Starr, D. F. Ogletree, H. Ogasawara, A. Nilsson, and M. Salmeron, J. Phys. Chem. C **111**, 8278 (2007).

[36]L. E. Walle, A. Borg, P. Uvdal, and A. Sandell, Phys. Rev. B **86**, 205415 (2012).

[37]J. Stöhr, *NEXAFS Spectroscopy* (Springer, Berlin/London, 2011).

[38]J. Knudsen, J. N. Andersen, and J. Schnadt, Surf. Sci. **646**, 160 (2016).

[39]F. J. Himpsel, F. R. McFeely, A. Taleb-Ibrahimi, J. A. Yarmoff, and G. Hollinger, Phys. Rev. B **38**, 6084 (1988).

[40]W. L. Jolly, K. D. Bomben, and C. J. Eyermann, At. Data Nucl. Data Tables **31**, 433 (1984).

[41]S. Y. Lee, C. Jeon, S. H. Kim, Y. Kim, W. Jung, K.-S. An, and C.-Y. Park, Jpn. J. Appl. Phys. **51**, 031102 (2012).

[42]M. Henzler, Appl. Surf. Sci. **11–12**, 450 (1982).

[43]S. O. Kucheyev *et al.*, Phys. Rev. B **69**, 245102 (2004).

[44]See supplementary material at https://doi.org/10.1116/1.5005533 for additional APXPS spectra.